

Degradable polycaprolactone nanoparticles stabilized via supramolecular host-guest interactions with pH-responsive polymer-pillar[5]arene conjugates

*Peng Wei,^{a,b} Fabian H. Sobotta,^{a,b} Carolin Kellner,^{a,b} Damiano Bandelli,^{a,b} Stephanie Höppener,^{a,b}
Stephanie Schubert,^{b,c} Johannes C. Brendel,^{a,b} Ulrich S. Schubert*,^{a,b}*

^aLaboratory of Organic and Macromolecular Chemistry (IOMC), Friedrich Schiller University Jena,
Humboldtstraße 10, 07743 Jena, Germany

^bJena Center for Soft Matter (JCSM), Friedrich Schiller University Jena, Philosophenweg 7, 07743
Jena, Germany

^cInstitute of Pharmacy and Biopharmacy, Department of Pharmaceutical Technology, Friedrich
Schiller University Jena, Lessingstrasse 8, 07743 Jena, Germany

*Correspondence to: U. S. Schubert (E-mail: ulrich.schubert@uni-jena.de)

ABSTRACT

Smart nano-carriers such as micelles, vesicles or nanoparticles constructed from amphiphilic polymers promise a new generation of drug delivery systems featuring localized and controlled release. Keeping the considerable effort for the synthesis of these polymers in mind, supramolecular host-guest interactions represent an interesting alternative to engineer amphiphilic materials with multiple functionalities. Using the known interaction of pillar[5]arenes with aromatic guests such as viologen-derivatives, we designed quasi-block copolymers based on polycaprolactone (PCL) and either the neutral and biocompatible poly(*N*-acryloyl morpholine) (PNAM-P[5]) or the structurally similar but pH-responsive poly(*N*-acryloyl-*N*'-methyl piperazine) (PNAMP-P[5]), which were modified with the pillar[5]arene. Self-assembly experiments in water resulted in the formation of

small spherical nanostructures for the methyl viologen-polycaprolactone (viologen-PCL), but surprisingly also for the non-functionalized PCL. However, only the pH-responsive PNAMP-P[5] gave stable structures in the buffer for both cases, while PNAM-P[5] resulted in aggregation. Additional degradation studies revealed that the presence of host-guest complexes could retard the disintegration of the particles at low pH (5.1) in comparison to the particles based on plain PCL, while all structures remained stable at neutral pH value. In combination with their excellent biocompatibility, the presented supramolecular approach to stabilize PCL nanoparticles with pH-responsive polymers pave a convenient way to degradable delivery systems with tailored release profiles.

KEYWORDS: amphiphilic polymers, pH-responsive, enzymatic degradation, supramolecular interactions

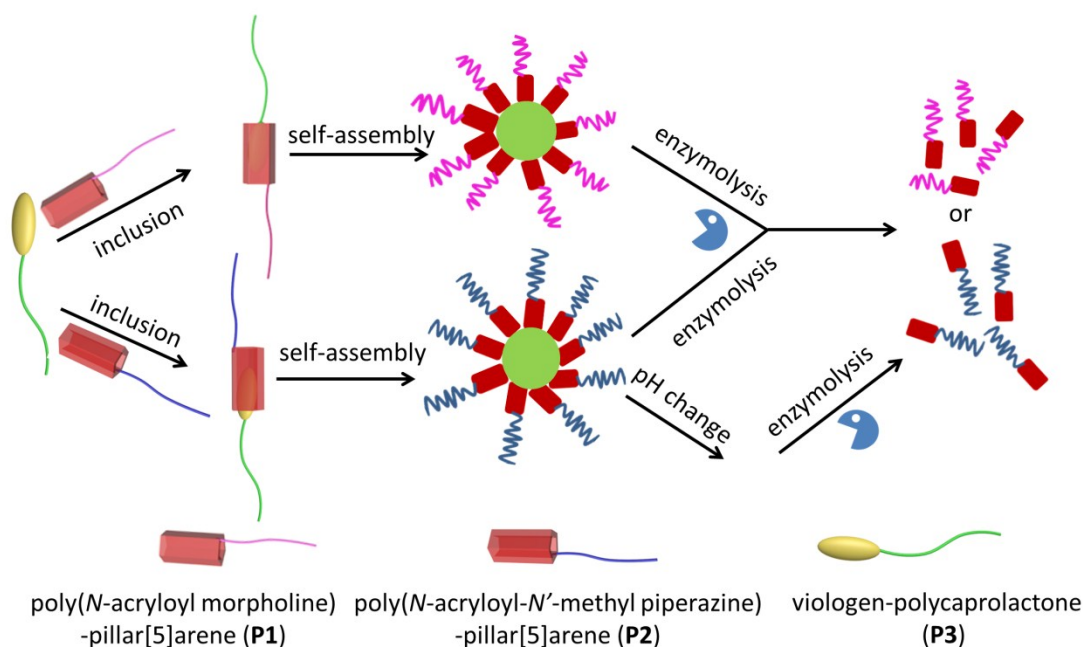
Introduction

In past decades, polymeric carriers including micelles, vesicles, nanotubes, nanogels, liposomes and capsules have attracted significant attention for their application in drug delivery, gene therapy, pharmaceuticals and tissue engineering.^{1, 2} Among them, polymeric micelles that are self-assembled from amphiphilic copolymers in water are recognized as one of the most promising nano-carrier systems. The hydrophobic part of the copolymer phase separates if transferred into water and provides as the core of the micelle a microenvironment for encapsulation of hydrophobic compounds such as drugs, and dyes etc., while the outer hydrophilic polymer acts as a shell, which stabilizes the micelles preventing precipitation and the clearance by the reticuloendothelial system (RES). This shielding effect further helps to prolong the circulation time in blood and to reduce their toxicity. Furthermore, the size of the micelles in the nanometer range can, for example, enhance the passive targeting into tumor tissue by the enhanced permeability and retention (EPR) effect.³⁻⁵

Stimulated by these properties, current research focuses in particular on smart and functional micelles, which do not only encapsulate and release hydrophobic compounds, but can for example react selectively to a local stimulus such as elevated temperature,^{6, 7} decreased pH value,⁸⁻¹⁰ different redox potential,^{11, 12} and the presence of enzymes.^{13, 14} So far, the general procedure relies on the synthesis of covalently linked hydrophilic and hydrophobic domains resulting in amphiphilic polymers, which subsequently self-assemble into micelles in water.¹⁵ In recent years, the development of selective and sufficiently strong supramolecular chemistry opened new possibilities to create amphiphilic quasi-block copolymers using non-covalent interactions.¹⁶ For example, crown ethers, cucurbiturils, or cyclodextrins represent typical macrocyclic motifs with a modifiable exterior and a hydrophobic cavity, which facilitates the selective inclusion of specific guest molecules. If both parts, the host and the guest, are selectively modified with hydrophobic or hydrophilic polymers, respectively, amphiphilic quasi-block copolymers are formed spontaneously by the resulting supramolecular interactions.¹⁷ Consequently, a variety of supramolecular polymer micelles have been prepared and studied for their resulting morphologies and responsive behaviors.^{16, 18, 19}

In recent years, pillar[n]arenes as a new generation of macrocyclic oligomers have attracted increasing attention because of their wide range of suitable guests that form strong inclusion complexes, as well as the option to conveniently modify their exterior.²⁰⁻²² These comparatively new supramolecular macrocyclic hosts have already demonstrated their potential for the fabrication of supramolecular assemblies.²³ Most of the work focused so far on modifications with small molecules but a few materials based on pillar[n]arenes have been demonstrated to form also amphiphilic polymers.²⁴⁻²⁶ In most cases, the resulting supramolecular assemblies based on pillar[n]arenes resulted in the formation of vesicles, which were considered for biomedical applications and, therefore, commonly modified with poly(ethylene glycol) (PEG) to induce good biocompatibility.²⁷⁻²⁹ Inspired by these reports, we wanted to explore the further potential of these host-guest interactions and the synthetic flexibility of the pillar[5]arene motif. Therefore, we modified the pillar[5]arene

selectively with one chain transfer agent (CTA) for the RAFT polymerization process, which enabled a versatile modification of this host with numerous vinyl monomers by the controlled radical polymerization process.^{30, 31} Having a non-toxic, non-ionic and biocompatible shell polymer in mind, we have chosen poly(*N*-acryloyl morpholine) (PNAM) as an interesting alternative to PEG.³² In addition, a structurally similar, but pH-responsive monomer *N*-acryloyl-*N'*-methyl piperazine (NAMP) was used to create a shell polymer (PNAMP), which remains mostly non-charged at neutral conditions, but becomes highly charged at low pH values (< 6). The latter is in particular interesting to test the robustness of the supramolecular interactions in micelles, as in the charged state strong repulsive forces are expected, which might break the interactions. For the hydrophobic core material, viologen modified polycaprolactone (viologen-PCL) was used to provide a biocompatible, enzymatically degradable, and non-toxic synthetic polymer, which is often used for drug carrier systems.^{33, 34} Overall, we compared the complexation ability of the resulting polymers, their self-assembly behavior, and the effect of the pH-responsive groups on the stability and degradation behavior of the materials (Scheme 1).



Scheme 1: Schematic representation of the complexation, self-assembly of polymers and degradation behaviors.

Experimental

Materials

Triethylamine, acryloyl chloride, azodiisobutyronitrile (AIBN), 1-(4-bromobutoxy)-4-methoxybenzene, sodium azide, acryloyl morpholine, ϵ -caprolacton, trifluoroacetic acid, and 4,4'-bipyridine were received from ABCR. All other chemicals were purchased from standard suppliers and used without further purification. Pillar[5]arene-modified CTA, polycaprolactone **P4**, viologen-modified-polycaprolactone **P3** and *N*-acryloyl-*N'*-methyl piperazine (NAMP) were synthesized according to literature procedures (NMR and SEC characterization is given in the SI, Figure S1-S8).^{28, 33, 35}

Instrumentation

¹H NMR spectra were recorded at room temperature on a Bruker Avance 300 MHz. The chemical shifts are given in ppm.

Size-exclusion chromatography (SEC) measurements were performed using an Agilent system (series 1200) equipped with a G1310A pump, a G1362A refractive index detector and a PSS GRAM column with DMAc (+ 0.21 wt.% LiCl) as eluent. The column oven was set to 40 °C, and a poly(methyl methacrylate) (PMMA) standard was used for calibration.

Dynamic light scattering (DLS) was performed on a Zetasizer Nano ZS (Malvern Instruments, Herrenberg, Germany). Suspensions of the materials (0.5 mg mL⁻¹) were measured at 25 °C or 37 °C ($\lambda = 633$ nm) at an angle of 173°. The size distribution of the spherical particles was calculated by applying the nonlinear least-squares fitting mode.

Transmission electron microscopy (TEM) was carried out on a FEI Technai G2 20 cryo-TEM. Samples were prepared with a Vitrobot Mark IV system. A total of 8 μ L of the sample solution (5 mg

mL⁻¹) was transferred onto Quantifoil (R2/2, Quantifoil) grids, which were cleaned by Ar plasma cleaning for 2 min prior to preparation. Samples were plunged into liquid ethane, transferred, and kept at temperatures below 170 °C by using a Gatan cryo-stage. Images were recorded with a Mega View G2 CCD camera (OSIS, 1392 × 1040 pixels) or an Eagle CCD camera (Eagle 4k HS 200 kV, 4096 × 4096 pixels).

Synthesis of pillar[5]arene-modified poly(*N*-acryloyl morpholine) (P1) and poly(*N*-acryloyl-*N*'-methyl piperazine) (P2)

The procedure for the synthesis of **P2** via RAFT polymerization is described here as an example: 800 mg NAMP, 82 mg pillar[5]arene-CTA and 1.2 mg AIBN (monomer/CTA/AIBN = 70/1/0.1) were dissolved in 2 mL anhydrous DMF in a Biotage microwave reaction vial. The reaction vial was degassed for 15 min by argon, then the flask was immersed in an oil bath under stirring at 70 °C overnight. The reaction was stopped by cooling to room temperature. The solution was diluted with 2 mL dichloromethane and subsequently precipitated into cool diethyl ether (three times). The yellow solid was dried under vacuum at room temperature for 24 hours. Subsequently, SEC and NMR (CDCl₃) were used to characterize their molar mass, dispersity and specific signals.

Complexation measurement by NMR and fluorescence titration

For the complexation measurement by NMR, either **P1** (4 mM), **P3** (4 mM) or **P1** (4 mM) + **P3** (4 mM) (or the same amount of **P2**, **P3** and **P2+P3** respectively) were dissolved in 550 μL acetone-*d*₆, and the proton NMR was measured at room temperature.

In order to study the association constant for the complexation between **P1** and **P3** (**P2** and **P3**), fluorescence titration experiments were conducted for the estimation of the association constant (*K*_a) in THF. By a molar ratio plot, 1:1 stoichiometry was obtained for the complexations. The non-linear curve-fittings were based on the following equation 1:

$$\Delta F = (\Delta F_{\infty}/[H]_0)(0.5[G]_0 + 0.5([H]_0 + 1/K_a) - (0.5([G]_0^2 + (2[G]_0(1/K_a - [H]_0) + (1/K_a + [H]_0)^2)^{0.5}))$$

ΔF is the difference in fluorescence intensity at 240 nm at $[H]_0$ (**P1** or **P2**), ΔF^∞ is the difference in fluorescence intensity at 240 nm when **P1** or **P2** is completely complexed. $[H]_0$ is the fixed initial concentration of **P1** or **P2** and $[G]_0$ is the initial concentration of **P3**.

Preparation of micelles

Nanoprecipitation was used to prepare the micelles. The preparation of **P1** and **P3** as an example was described as below: 6 mg **P1** and 1 eq. (4 mg) **P3** were first dissolved in 1.7 mL acetone, which was subsequently stirred for 1 hour at room temperature to allow the formation of the complex. Afterward, the solution was dropped slowly into 10 mL water or buffer solution using a syringe-pump at a speed of 0.1 mL min⁻¹. After removal of the acetone by evaporation overnight at room temperature, the micelles were examined by DLS and TEM.

CMC-determination

The critical micelle concentration (CMC) was determined using Nile Red as a fluorescence indicator.³⁶ A stock solution ($c = 1 \text{ mg mL}^{-1}$) of corresponding micelles was diluted to serials of samples with decreasing concentrations. Then, 5 μL of a Nile Red solution (1 mg mL^{-1} in THF) was added and the samples were stirred openly for 20 h at room temperature in the dark. Subsequently, the fluorescence intensity of Nile Red was measured using the Tecan Plate Reader (samples were placed in a 96 glass well plate) and applying an excitation wavelength of 549 nm. The CMC was calculated as the intercept of the two resulting linear fits in the plot of emission intensity *versus* $\log c$.

pK_a determination by titration experiments

The pK_a value of **P2** was measured according to potentiometric titration by using sodium hydroxide. Briefly, 10 mL of **P2** solution at 1 mg mL^{-1} was first adjusted to acidic condition (pH 2.8) by 0.1 M HCl. The titrant (NaOH, 0.1 M) was added at a flow rate of 0.05 mL min⁻¹. The pH value of the solution corresponding to the volume of titrant was derived from the raw titration data, which was recording by titration automation (Metrohm, Switzerland). The pK_a of **P2** was determined by the

mean value of pH of the two maxima of the first equivalence point recognition criterion (EPR) of this function according to the Henderson-Hasselbalch equation 2:

$$pH = pK_a + \log \frac{[A^-]}{[HA]}$$

Then, the degree of charge (α) of **P2** at different pH values was calculated using the pK_a according to equation 3:

$$\alpha = \frac{1}{10^{pK_a - pH} + 1}$$

Analysis of response to changes in pH value

0.5 mL of the micelle suspension (1 mg mL⁻¹) was diluted with 0.5 mL of buffer solution (phosphate buffer at pH 7.4 or 6.3, and acetate buffer at pH 5.1 or 4.2) and stirred for additional 30 min at 37 °C. Afterward, the size, mean count rate and zeta potential of the resulting solutions were measured by DLS. For the titration experiment, 5 mL of the micelle solution (0.5 mg mL⁻¹) was prepared in water. Diluted HCl or NaOH solutions (0.1 mM) were used to adjust the pH value. At each tested pH value, aliquots (0.5 mL) were taken and analyzed by DLS for the determination of their size and mean count rate.

Degradation studies

0.5 mL of the micelle suspension (1 mg mL⁻¹) was mixed with a PBS solution (phosphate buffer at pH 7.4 or acetate buffer at pH 5.1) with or without *Candida rugosa* lipase enzyme (1 U mL⁻¹) and incubated at 37 °C. At each time point, aliquots of 0.5 mL were taken to measure the size and mean count rate by DLS.

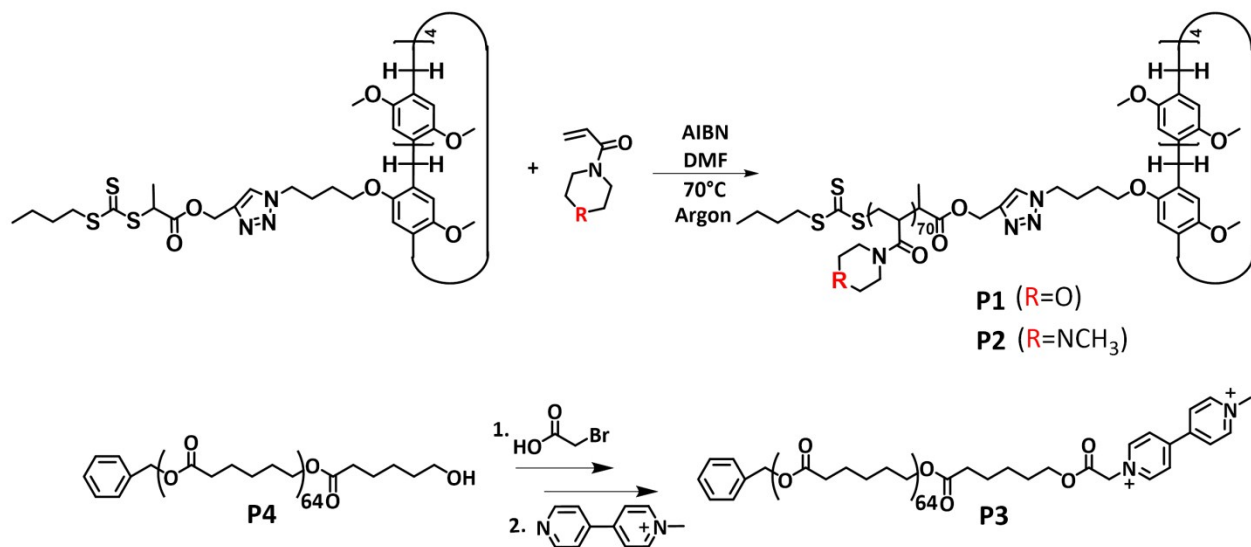
Cytotoxicity

Cytotoxicity studies were performed with the mouse fibroblast cell line L929 (CCL-1, ATCC), as recommended by ISO10993-5. The cells were routinely cultured in Dulbecco's modified eagle's

medium (DMEM, Biochrom, Germany) supplemented with 10% fetal calf serum (FCS, Capricorn Scientific, Germany), 100 U mL⁻¹ penicillin and 100 µg mL⁻¹ streptomycin at 37 °C (Biochrom, Germany) in a humidified 5% (v/v) CO₂ atmosphere. The cells were seeded at 1 × 10⁴ cells per well in a 96-well plate and incubated for 24 h. No cells were seeded in the outer wells. Afterward, both polymer suspensions were added to the cells in fresh media at indicated concentrations (from 50 to 500 µg mL⁻¹) and the plates were incubated for 24 h. Control cells were incubated with fresh culture medium and 10% NaCl (dilution buffer). Subsequently, the media was replaced by a mixture of fresh culture medium and PrestoBlue (resazurin based solution, Thermo Fisher, Germany, prepared according to the manufacturer's instructions). After further incubation for 45 min at 37 °C in a humidified 5% (v/v) CO₂ atmosphere, the fluorescence was measured at Ex 560 nm/Em 590 nm, with untreated cells on the same well plate serving as negative controls. The negative control was set as 0% of metabolism inhibition and referred to as 100% viability. Data are expressed as mean ± standard deviation (SD) of three independent determinations of six data points each.

Results and Discussion

Synthesis of polymers



Scheme 2: Schematic representation of synthesis routes to all polymers.

The polycaprolactone (PCL) polymers **P4** (control without viologen unit) and **P3** (viologen end group) were synthesized according to procedures reported in literature (Scheme 2).^{28, 33} The hydrophilic polymers poly(*N*-acryloyl morpholine)-pillar[5]arene (PNAM-P[5], **P1**) and poly(*N*-acryloyl-*N*-methyl piperazine)-pillar[5]arene (PNAMP-P[5], **P2**) were both synthesized by reversible addition-fragmentation chain transfer (RAFT) polymerization with AIBN as initiator (Scheme 2).³⁷ The chain transfer agent (CTA) was synthesized according to published similar procedures connecting an azide modified pillar[5]arene with an alkyne modified trithiocarbonate in a copper-catalyzed azide-alkyne cycloaddition (CuAAC) (SI, Scheme S1).³⁸ The pillar[5]arene represents a suitable host for the complexation of the viologen moiety in **P3**. All polymers were characterized by ¹H NMR spectroscopy and SEC and featured narrow distributions ($D < 1.2$) (Table 1, SI, Figure S2-S7). The ¹H NMR spectrum further confirmed the successful end group modification of **P1**, **P2** and **P3** as all representative signals of either the pillar[5]arene or the viologen units were observed in the corresponding spectra after purification (SI, Figure S2, S3).

Table 1: Overview of selected characteristics of the polymers.

Abbrev.	DP (NMR) ^a	M _n (NMR) (g mol ⁻¹)	M _n (SEC) ^d (g mol ⁻¹)	M _w (SEC) (g mol ⁻¹)	<i>D</i>
P1	70 ^b	11,000	9,600	10,600	1.10
P2	70 ^b	11,900	9,600	11,500	1.19
P3	64 ^c	7,700	10,700	11,200	1.04
P4	64 ^c	7,400	10,700	11,100	1.04

^a Determined from ¹H NMR analysis. ^b Calculated from the signal intensity of the proton on the pillar[5]arene ($\delta = 6.5$ ppm) in comparison to the proton signal of the hexa-atomic ring of polymers ($\delta = 3.5$ ppm). ^c Calculated from the signal intensity of the proton on the benzene ring ($\delta = 6.5$ ppm) in comparison to the proton signal of the methylene connected with the acyl group of polymers ($\delta = 4.1$ ppm). These ratios were used to calculate the DP. ^d SEC: DMAc + 0.21 wt.% LiCl, poly(methyl methacrylate) (PMMA) calibration.

Host-guest complexation

The complexation of the respective polymer components (*e.g.* **P2** and **P3**) is crucial for the successful preparation of the quasi-block copolymers. ¹H NMR was chosen as the general method to confirm the complexation.³⁹ In the corresponding spectrum (Figure 1), signals **a**, **b**, **c** and **d** belong to the viologen moiety, which disappears if the complex with the pillar[5]arene is formed. Similarly the signal **1** for the pillar[5]arene becomes broader in the mixture, which also confirmed a successful complexation. Interestingly, mixing the neutral polymer **P1** and **P3** did not result in the full disappearance of the signals for the viologen in the ¹H NMR spectra, which is most likely related to a weaker complexation ability of **P1** compared to **P2** (SI, Figure S8). The origin of this difference remains unclear, as in both cases the same pillar[5]arene is used. We can only assume that the difference in the monomer structure might change the coiling of the polymer chains, which affects the accessibility of the cavity in the host.

In order to analyze this complexation strength of **P1+P3** and **P2+P3**, titration experiments were performed, where the change of fluorescence intensity of the pillar[5]arene was monitored. For this purpose, increasing amounts of **P3** were constantly added to a solution of a fixed concentration of **P1** or **P2** in accordance with reported procedures.²⁷ Due to the complexation between pillar[5]arene and the viologen moiety, the fluorescence of the first got quenched with the addition of **P3**. According to **equation 1**, the associate constants (K_a) of **P1+P3** and **P2+P3** were calculated to be $(3.55\pm 0.22) \times 10^4 \text{ M}^{-1}$ and $(9.3\pm 0.49) \times 10^4 \text{ M}^{-1}$ respectively (SI, Figure S9, S10). These results confirm our previous assumption that the complexation strength of **P2+P3** is higher compared to **P1+P3**.

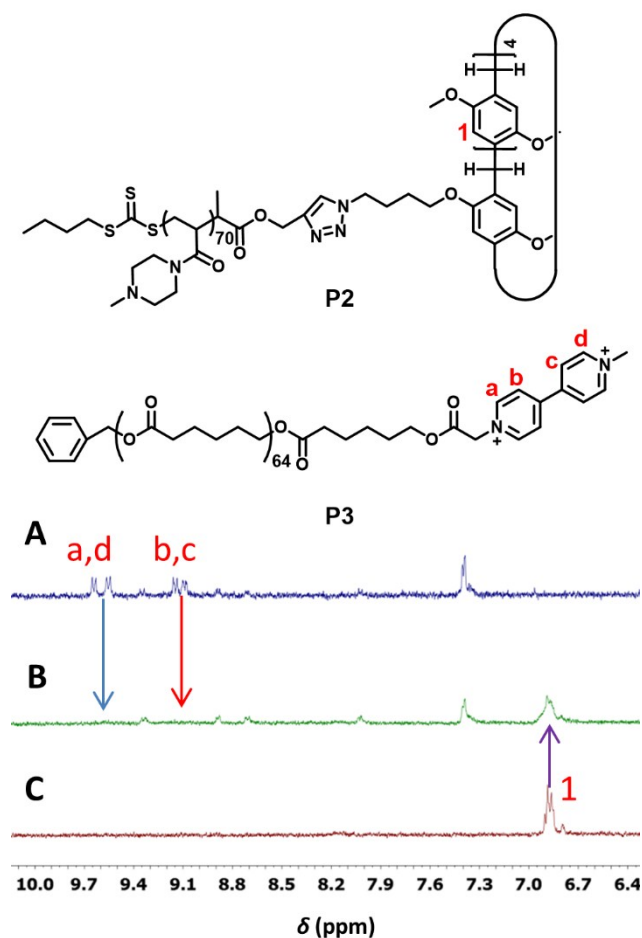


Figure 1 ^1H NMR (acetone- d_6 , 300 MHz, 25 °C) spectra of A) 4 mM **P3**, B) complex of **P3** (4 mM) with 1 eq. **P2**, C) **P2** (4 mM).

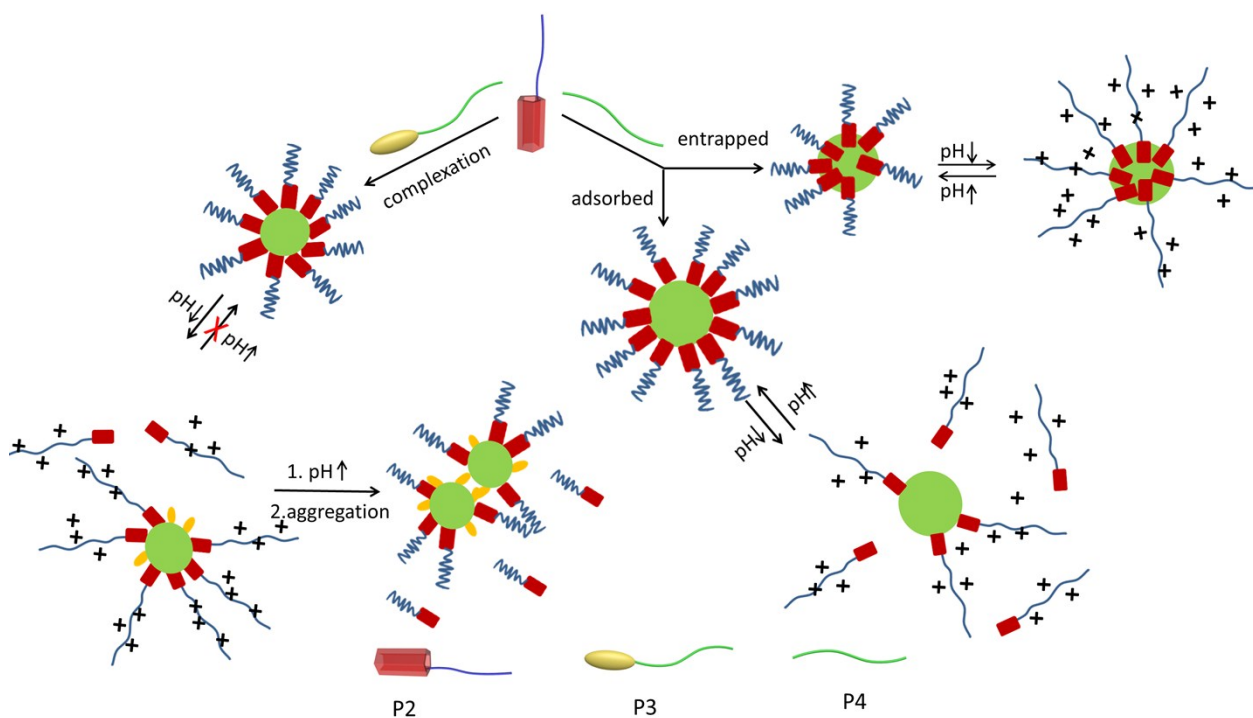
Preparation and analysis of nanostructures in aqueous media

Nanoprecipitation was used to prepare micelles or nanoparticles in aqueous solution.^{40, 41} This method provides excellent reproducibility without tedious processing steps. In this process, both polymers (host and guest modified) were first dissolved in acetone and stirred for 1 h to ensure the formation of the complex and consequently an amphiphilic quasi-block copolymer. Subsequently, the solution was continuously and slowly added into H₂O using a syringe-pump (0.1 mL min⁻¹), which causes the insoluble polymer to phase separate, but as it is bound to the soluble polymer by the host-guest complex, micellar structures are formed, similar to covalently linked amphiphilic block copolymers (see Scheme 1). The solution was finally stirred at room temperature to let all the remaining acetone evaporate. The dropping into water causes a rather rapid change of the environment, which might cause the formation of kinetically trapped stages. As we do not expect a further dynamic exchange, we preferred the more general term nanostructure in the following.⁴²

As listed in Table 2, stable nano-sized micelles were obtained in pure aqueous solution for the neutral polymer **P1** as well as the pH-responsive polymer **P2** in combination with **P3** (viologen-PCL). Interestingly, even similar nanostructures are formed using only the viologen modified PCL (**P3**), which might be stabilized by the permanent cationic charges on the viologen unit. However, an unmodified PCL **P4** also yielded nano-sized particles but displayed a slightly increased size (64 nm). The combination of **P2** containing pillar[5]arene units and **P4** (PCL) also gave narrowly distributed nanostructures that even further increased in size (90 nm).

While all nanostructures seem to be stable in pure water, we further tested buffered saline solutions, which are commonly used for biological experiments and crucial for the later mentioned degradation tests. To our surprise, the micelles formed with the polymers **P3** (viologen-PCL) and the neutral **P1** aggregated rather quickly in PBS buffer (in less than one day) (Figure S11, SI), while such behavior was expected for the pure PCL based nanoparticles, if they are not stabilized.^{43, 44} This unexpected behavior in comparison to other reported neutral polymers might correlate with the previously observed weaker complexation strengths of **P1**. As a consequence, the host-guest complex might be

destabilized during the assembly as the PNAM chains are forced to stretch. Due to this increased steric demand in the shell of the nanostructure PNAM chains may be released, which resulted in a decreased stability of the nanoparticles. On the contrary, the structures prepared from **P2** and **P3** remain stable in PBS and give particles of similar size (41 nm) as for pure water. To verify the stability of the complex even in presence of the buffer, we examined them by ^1H NMR spectroscopy. Despite a very low signal intensity, the disappearance of the signals for the viologen-PCL prove their stability in water as well as PBS (SI, Figure S12).



Scheme 3: Schematic representation of the complexation and self-assembly of **P2+P3** and **P2+P4** and their pH-sensitive behavior.

Initially thought as a control experiment, we also tested **P4** (PCL), which does not contain viologen for complexation. While in pure water this combination (**P4** + **P2**) formed nanostructures (90 nm), which are even slightly larger compared to the pure **P4**, we expected it to precipitate in buffer solution as all other non-modified polymers. However, a stable dispersion with similar size (85 nm) and dispersity as for pure water was observed, which is in particular surprising considering the strong

tendency to aggregate even when complexed with **P1** (PNAM) and **P3** (viologen-PCL). Some reports mention that similar PCL can be included in the used pillar[5]arene, and we therefore examined the resulting structures from **P2** and **P4** by ^1H NMR (SI, Figure S13). However, no shifts of any peaks or disappearance of signals was observed as it is described in the referred literature which indicates the absence of complexes between PCL and the pillar[5]arene in our case.⁴⁵⁻⁴⁷ Thus, we assume that the strong hydrophobicity of pillar[5]arene in combination with the hydrophilic and maybe even slightly charged **P2** is able to stabilize the nanoparticle formed by **P4** in the core, which has so far only been reported for block copolymers.⁴⁸ In other words, the pillar[5]arene of **P2** is incorporated into the hydrophobic domain formed by **P4**, while the hydrophilic PNAMP can stabilize the overall structure (Scheme 3). Further studies on the critical aggregation concentration (CAC) revealed low values ($47\ \mu\text{g mL}^{-1}$ for **P2+P3**, $30\ \mu\text{g mL}^{-1}$ for **P2+P4**) for both combinations (viologen-PCL and PCL) with the pH-responsive polymer PNAMP (SI, Figures S14 and S15). Keeping a potential application in nanomedicine in mind, we also investigated the stability of these nanoparticles during incubation in a cell culture medium. Both **P2+P3** and **P2+P4** demonstrated excellent stability without any sign of aggregation over 48 h (SI, Figure S16).

The resulting morphologies of these nanoparticles were examined with TEM or cryo-TEM (Figure 2, SI, Figure S17). The size of the micelles based on **P2** (PNAMP) and **P3** (viologen-PCL) ranged from 20 to 70 nm, while nanoparticles constructed from **P2** (PNAMP) and **P4** (PCL) exhibited a size range of 50 to 200 nm, which can be expected to take their distribution (PDIs 0.21 and 0.23) into account. In the latter case, the particles appear rather bright in their center, which might indicate hollow structures, but this appearance is more likely due to drying effects and a collapse of the shell around the PCL core in the dried TEM sample.

Table 2: Summary of the characteristics of the different nanostructures.

Abbrev.	H₂O		PBS	
	Z-Ave (nm)	PDI	Z-Ave (nm)	PDI
P1+P3	33	0.34	Aggregation	
P2+P3	43	0.23	41	0.13
P2+P4	90	0.21	85	0.15
P3	44	0.36	Aggregation	
P4	64	0.15	Aggregation	

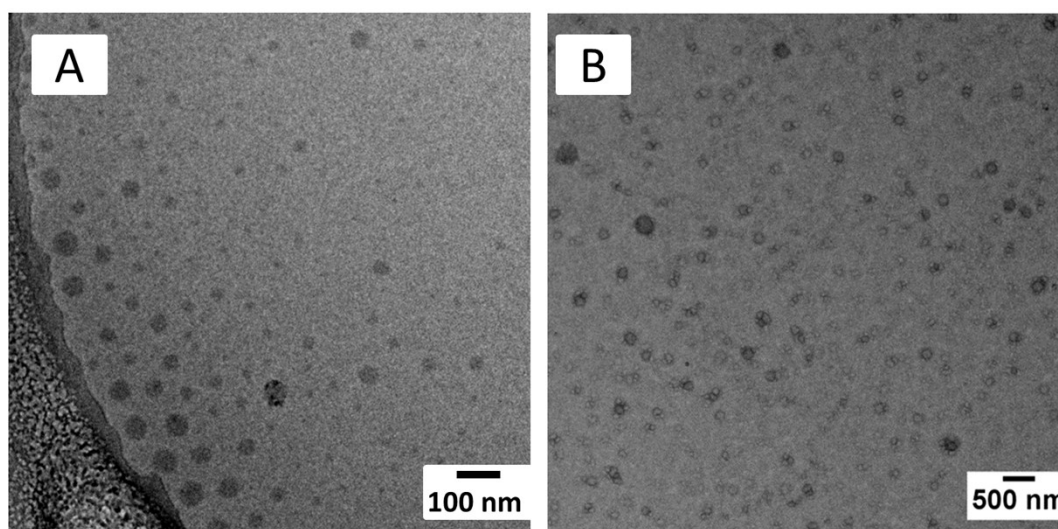


Figure 2 A) cryo-TEM image of **P2 + P3**, B) TEM image of **P2 + P4**.

Response to pH-changes

As the polymer **P2** (PNAMP) features tertiary amino groups, it can be protonated or deprotonated depending on the pH value of the surrounding media. To estimate the degree of charge and the corresponding acid dissociation constant (pK_a), titration experiments were first performed on the pure polymer (see SI for further details, Figures S18, S19). The resulting pK_a of **P2** was 5.2, which means that almost all of the amino groups are deprotonated at a physiological pH of 7.4. The corresponding micelles formed by **P2** as shell material might differ slightly from this behavior but should follow a

similar trend. As a consequence, the micelles prepared from **P2** (**P2+P3** and **P2+P4**) were all tested for their response to pH changes in the relevant range between 4 and 7.4. As shown in Figure 3, the zeta potentials of both micelles increased with decreasing pH value with the most significant changes occurring between a pH of 6.3 and 5.1, which is around the pK_a of the homopolymer. This change in the zeta potential of the micelle certainly confirmed the increasing number of charged units on the surface of the micelle, but on the contrary the increasing charge repulsion might cause the dissociation of the complexes formed by **P2** and **P3** or a detachment of the stabilizing shell in the combination of **P2** and **P4**. To elucidate these possibilities, the stability, size and distribution of both micelles were examined by DLS at various pH values (Figure 4). In both cases, an initial increase in size can be observed with decreasing pH (black numbers and line, points 1 to 7), which are more pronounced for the host-guest complex-forming polymers **P2+P3**. Such an increase in size has already been reported for amino-functionalized block copolymer micelles, and is related to the increased stretching of the shell polymers due to charge repulsion.⁴⁹ We assume a similar effect in our case, which has a more significant influence on the smaller micelles of 43 nm (**P2+P3**) in contrast to the larger nanoparticles of 90 nm (**P2+P4**). On the other hand, the count rate decreases in both cases, but not to the extent that a dissolution of the nanostructures can be concluded. The observed reduction might be more related to the decreased density of the shell due to the increased uptake of water, which influences the scattering intensity (Scheme 3). Notably, the dispersity of the micelle formed by **P2** and **P3** increased significantly (from 0.13 to > 0.4) with lower pH (points 1 to 7), which might be correlated to an uncontrolled aggregation of some nanoparticles, while this effect is not observed for **P2+P4**. In addition, **P2+P3** did result in larger structures with broader distribution when reversing the acidification by the addition of sodium hydroxide (points 7 to 11) and returning to a neutral pH value of around 7.5. On the contrary, no significant difference was observed for the nanoparticles made with **P2** and **P4** before and after these acidification and neutralization steps. We assume that the strong repulsive force created by the increasing charge density on the polymers **P2** led to a partial disintegration of the host-guest complexes, which are most likely located at the

surface of the micelle. When returning to neutral pH conditions, less stabilizing chains remained on the surface of the nanoparticles, which subsequently led to partial aggregation (Scheme 3). In the case of the nanostructures formed by **P2+P4** we believe the hydrophobic pillar[5]arene moiety is buried in the solid hydrophobic domain of the nanoparticles and, therefore, locked into the PCL core preventing the dissolution of the **P2** chains from the surface (Scheme 3). Another explanation might also be a faster resorption of **P2** onto the **P4** nanoparticles when reducing the charge density or the repulsive forces, respectively, while the reformation of the complexes between the pillar[5]arene (**P2**) and the viologen unit on **P3** might be kinetically hindered on the limited surface of these smaller micelles (Scheme 3).

A further point that should be considered is the formation of NaCl during the whole process. The salt could cause a screening of the repulsive Coulomb interactions, which might contribute to the instability of the nanostructures formed by **P2+P3**. In case of **P2+P4** we do not observe any difference, which again might be due to the kinetical trapping of PNAMP on the surface or a fast re-adsorption. We nevertheless attribute only a minor effect of the salt to this behavior as both nanostructures remain stable and give similar sizes in PBS, which has certainly higher salt concentrations (see Table 2).

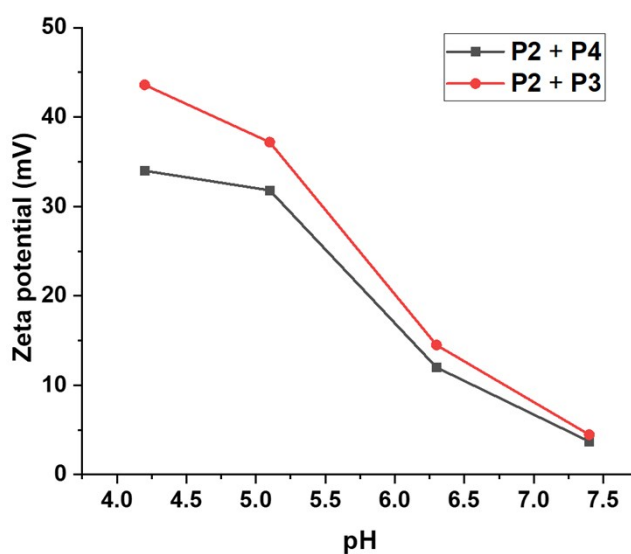


Figure 3: Zeta potential of A) **P2+P4** and B) **P2+P3** at different pH values measured by DLS.

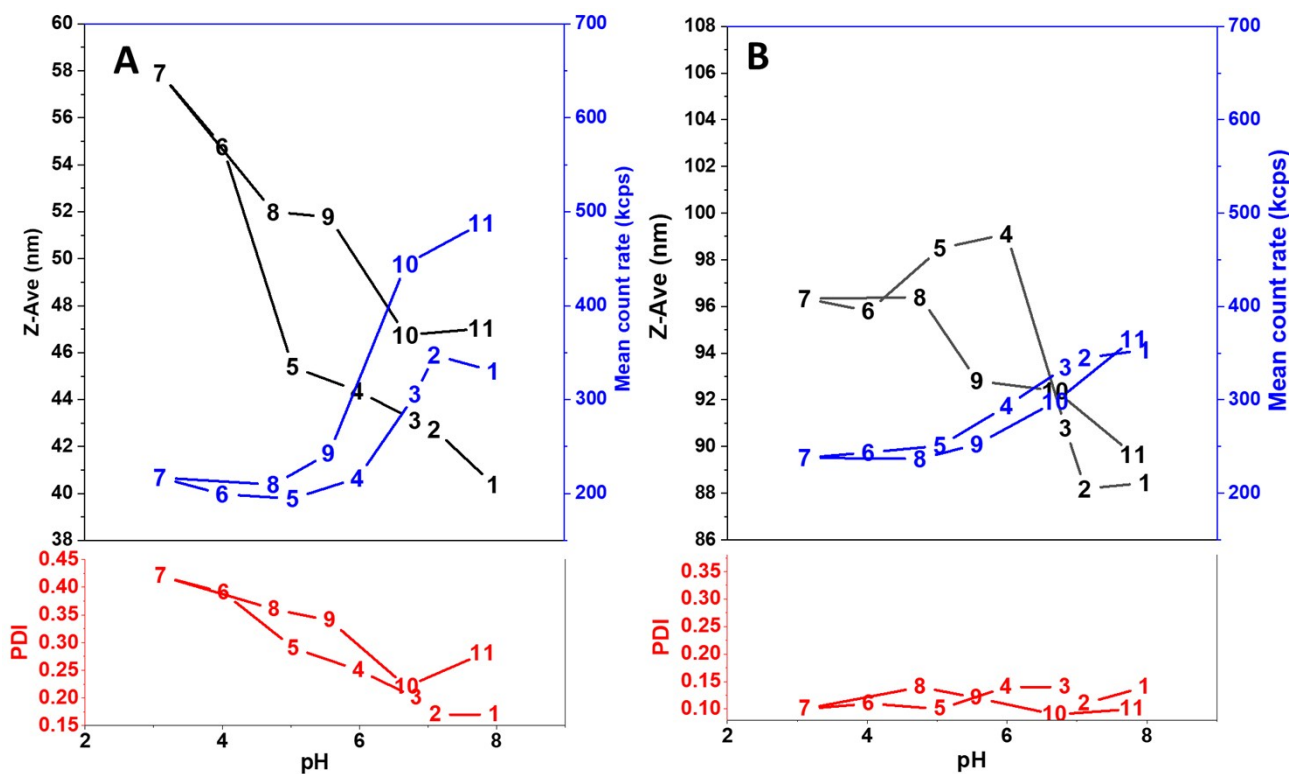


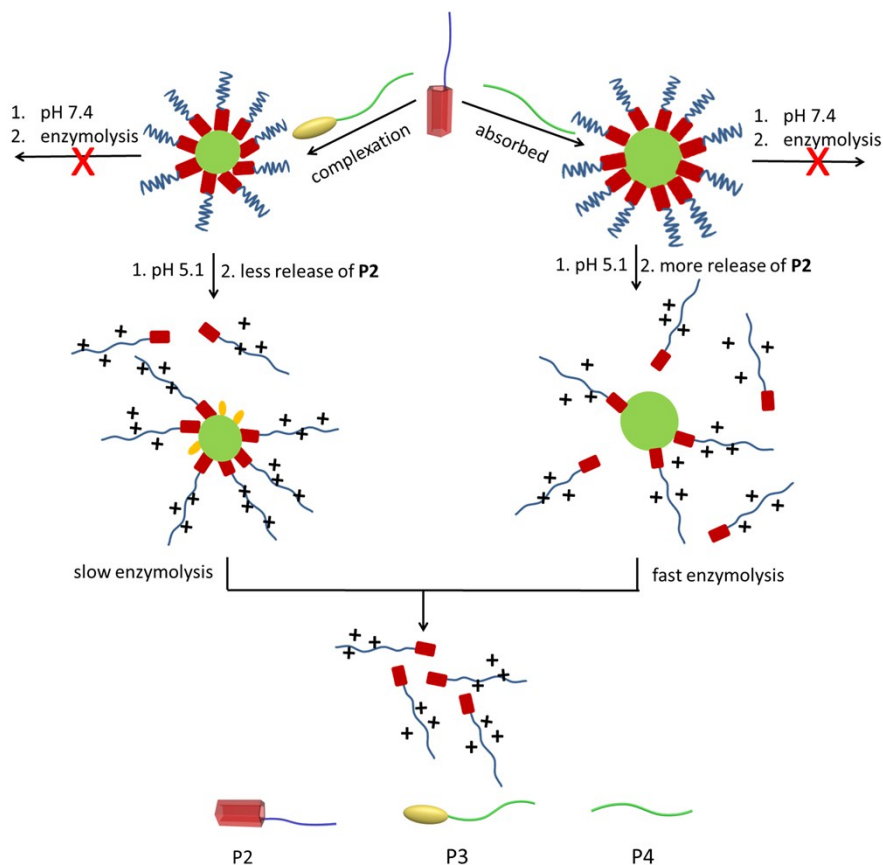
Figure 4: DLS results of A) **P2+P3** and B) **P2+P4** at different pH values.

Degradation study

In addition to stability tests at various pH values, we further examined the degradation behavior at neutral and acidic conditions as they would appear in the endo/lysosomal uptake pathway.⁵⁰ PCL is a well-known biocompatible and biodegradable material, which has already been used in a large variety of nano-carrier systems.^{34, 51} Its biodegradation can be triggered by pH changes and in the presence of enzymes.⁵²⁻⁵⁴

In this work, we tested both the degradation behavior of the nanostructures at physiological and acidic pH values and in the presence of the enzyme *Candida rugosa* lipase, which is known to degrade PCL (Scheme 4).⁵⁵ As only **P2+P3** and **P2+P4** did not aggregate in the buffer, we focused on these systems. Therefore, the particles are incubated either at physiological neutral conditions (pH

7.4) or acidic conditions (pH 5.1) with or without enzyme, respectively. The temperature was kept at 37 °C, and the count rate as an indicator for the number of remaining particles was monitored by DLS for two days. All the micelles remained stable at pH 7.4 even in the presence of *Candida rugosa* lipase enzyme. Furthermore, at pH 5.1 no sign of degradation can be observed in the absence of the enzyme demonstrating a stabilizing effect of the shell (SI, Figure S20). Previous reports also describe slow degradation.^{54, 56} However, in the presence of the enzyme the particles degrade at these acidic conditions. Such an influence of pH value on the enzymatic activity for PCL has previously already been reported.⁵⁷ Interestingly, the degradation rate differs quite significantly for the nanostructures formed by **P2+P4** compared to **P2+P3**. For the first system, a very rapid decay within the first hours is observed, while the latter demonstrates a more continuous degradation profile over several hours. For **P2+P3**, the remaining complexes formed by the pillar[5]arene (**P2**) and the viologen attached to the PCL (**P3**) might impede the accessibility of enzyme to the core materials and, consequently, retard the degradation process. In the case of **P2+P4** we assume that more PNAMP chains (**P2**) got detached at the reduced pH value and the increasing coulombic repulsion, which unveils the PCL (**P4**) to the enzyme and accelerates the degradation process (Scheme 4). In a further experiment we varied the content of the viologen units to examine whether the observed stabilization effect is influenced and the resulting degradation rate can be tuned. Therefore, 0.5 eq. **P4** (PCL) and 0.5 eq. **P3** (viologen-PCL) were mixed and combined with the pillar[5]arene modified **P2** previous to the preparation of the nanoparticles. This combination, first of all, resulted in well-defined particles with a diameter between the particles formed by **P2+P3** or **P2+P4** (SI, Figure S21). Moreover, the obtained degradation rate (Figure 5, pH 5.1) is enhanced compared to **P2+P3**, which supports our assumption that the stability can be tuned with the content of host-guest complexes.



Scheme 4: Schematic representation of the enzymatic degradation behaviors of **P2+P3** and **P2+P4** at different pH values.

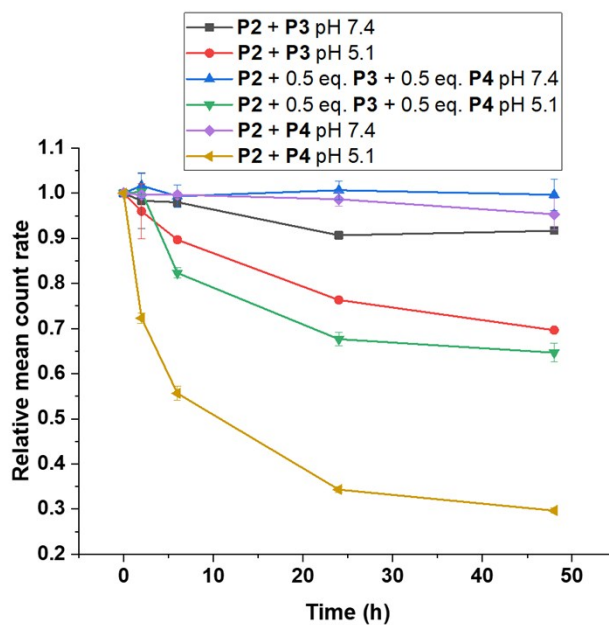


Figure 5: Count rate measurements (DLS) to monitor the enzymatic degradation (1 U mL^{-1}) at different pH values.

Cytotoxicity of nanoparticles

Many cationic polymers or nanoparticles are known to induce severe toxic effects in cells due to their interactions with the negatively charged cell membranes. Therefore, the cytotoxicity of the presented nanoparticles was investigated using the cell line L929.⁵⁸ In addition, the pure polymer **P2** was tested as a control. The pure PCL polymers however aggregate in the used media and were, therefore, not considered as controls. Despite the presence of the potentially cationic units on the polymer **P2**, both the free polymer and the nanostructures formed from **P2+P3**, as well as **P2+P4** display similar non-toxic characteristics (Figure 6), which confirmed their biocompatibility even at high concentrations. The low cationic charge density of the corresponding nanoparticles might not be substantial under physiological conditions (pH 7.4) and therefore have no detrimental effect can be observed.

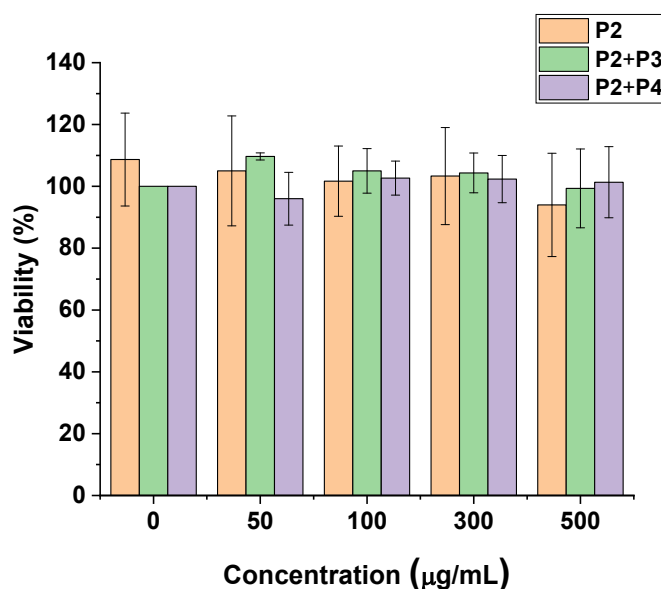


Figure 6: PrestoBlue assay to evaluate the cytotoxicity of the nanoparticles that were prepared from **P2**, **P2+P3** and **P2+P4** respectively.

Conclusion

In summary, the presented study demonstrates that the pillar[5]arene represents a promising motif for the formation of amphiphilic quasi-block copolymers, which can be assembled into stable nanostructures. Using the RAFT process and using a pillar[5]arene modified chain transfer agent, we

have prepared a well-defined poly(*N*-acryloyl morpholine) (PNAM), which is a known alternative to PEG, and a pH-responsive analog poly(*N*-acryloyl-*N'*-methyl piperazine) (PNAMP), which features protonable tertiary amino groups. These materials were subsequently combined with polycaprolactones, which was in one case modified with the common guest molecule viologen. Surprisingly, PNAMP gave stable nanostructures in buffer or cell media, while the neutral polymer PNAM resulted in aggregation. Moreover, even pristine PCL could be stabilized by the pillar[5]arene modified PNAMP, which could be related to a hydrophobic interaction of the pillar[5]arene with the PCL. While all prepared nanostructures increase in size at lower pH values, the return to neutral conditions resulted in an aggregation of the nanostructures formed by the viologen modified PCL although no significant change was observed for the pristine PCL. We assume that in both cases PNAMP chains were expelled from the surface due to the strongly repulsive electrostatic forces, but the hydrophobic interactions in the latter case might be more reversible. The reformation of the host-guest complex between the pillar[5]arene PNAMP and the viologen-PCL might further be kinetically hindered. Subsequent enzymatic degradation tests on these materials further revealed that the particles formed by pristine PCL (no complex) degraded rapidly, while the host-guest complex in the case of viologen-PCL induces a more continuous degradation profile. By combination of the different PCL materials (with and without viologen moiety) we could further prove that the degradation rate can be tuned. In combination with their high biocompatibility, the presented combination of materials represents a versatile route to functional nanocarriers with controlled degradation profile, while circumventing tedious synthesis steps required for the preparation of equivalent block copolymers.

Notes

The authors declare no competing financial interest.

Acknowledgements

P. W. was financially supported by the China Scholarship Council. J. C. B. and F. H. S. acknowledge the Deutsche Forschungsgemeinschaft (DFG) for generous funding within the Emmy-Noether-Programme (Project-ID: 358263073). We further acknowledge funding from the collaborative research center PolyTarget (project number 316213987, SFB 1278, projects A04, A06, C01, Z01) by the DFG. Transmission electron microscopy studies were conducted in the Electron Microscopy facilities of the Jena Center for Soft Matter, which have been established by grants from the DFG and the European Funds for Regional Development (EFRE).

References

1. Mai, Y.; Eisenberg, A., Self-assembly of block copolymers. *Chem. Soc. Rev.* **2012**, *41*, 5969-5985.
2. Molina, M.; Asadian-Birjand, M.; Balach, J.; Bergueiro, J.; Miceli, E.; Calderón, M., Stimuli-responsive nanogel composites and their application in nanomedicine. *Chem. Soc. Rev.* **2015**, *44*, 6161-6186.
3. Cabral, H.; Miyata, K.; Osada, K.; Kataoka, K., Block copolymer micelles in nanomedicine applications. *Chem. Rev.* **2018**, *118*, 6844-6892.
4. Elsabahy, M.; Wooley, K. L., Design of polymeric nanoparticles for biomedical delivery applications. *Chem. Soc. Rev.* **2012**, *41*, 2545-2561.
5. Nicolas, J.; Mura, S.; Brambilla, D.; Mackiewicz, N.; Couvreur, P., Design, functionalization strategies and biomedical applications of targeted biodegradable/biocompatible polymer-based nanocarriers for drug delivery. *Chem. Soc. Rev.* **2013**, *42*, 1147-1235.
6. Nakayama, M.; Okano, T.; Miyazaki, T.; Kohori, F.; Sakai, K.; Yokoyama, M., Molecular design of biodegradable polymeric micelles for temperature-responsive drug release. *J. Controlled Release* **2006**, *115*, 46-56.
7. Sun, X.-L.; Tsai, P.-C.; Bhat, R.; Bonder, E.; Michniak-Kohn, B.; Pietrangelo, A., Thermoresponsive block copolymer micelles with tunable pyrrolidone-based polymer cores: structure/property correlations and application as drug carriers. *J. Mater. Chem. B* **2015**, *3*, 814-823.

8. Tong, H.; Wang, Y.; Li, H.; Jin, Q.; Ji, J., Dual pH-responsive 5-aminolevulinic acid pseudopolyrotaxane prodrug micelles for enhanced photodynamic therapy. *Chem. Commun.* **2016**, 52, 3966-3969.
9. Zhou, X. X.; Jin, L.; Qi, R. Q.; Ma, T., pH-responsive polymeric micelles self-assembled from amphiphilic copolymer modified with lipid used as doxorubicin delivery carriers. *R. Soc. Open Sci.* **2018**, 5, 171654.
10. Chen, L.; Chen, B.; Liu, X.; Xu, Y.; Zhang, L.; Cheng, Z.; Zhu, X., Real-time monitoring of a controlled drug delivery system in vivo: construction of a near infrared fluorescence monomer conjugated with pH-responsive polymeric micelles. *J. Mater. Chem. B* **2016**, 4, 3377-3386.
11. Huo, M.; Yuan, J.; Tao, L.; Wei, Y., Redox-responsive polymers for drug delivery: from molecular design to applications. *Polym. Chem.* **2014**, 5, 1519-1528.
12. Sang, X.; Yang, Q.; Shi, G.; Zhang, L.; Wang, D.; Ni, C., Preparation of pH/redox dual responsive polymeric micelles with enhanced stability and drug controlled release. *Mater. Sci. Eng. C* **2018**, 91, 727-733.
13. Hu, J.; Zhang, G.; Liu, S., Enzyme-responsive polymeric assemblies, nanoparticles and hydrogels. *Chem. Soc. Rev.* **2012**, 41, 5933-5949.
14. Harnoy, A. J.; Slor, G.; Tirosh, E.; Amir, R. J., The effect of photoisomerization on the enzymatic hydrolysis of polymeric micelles bearing photo-responsive azobenzene groups at their cores. *Org. Biomol. Chem.* **2016**, 14, 5813-5819.
15. Fuks, G.; Talom, R. M.; Gauffre, F., Biohybrid block copolymers: Towards functional micelles and vesicles. *Chem. Soc. Rev.* **2011**, 40, 2475-2493.
16. Zou, H.; Yuan, W.; Lu, Y.; Wang, S., UV light-and thermo-responsive supramolecular aggregates with tunable morphologies from the inclusion complexation of dendritic/linear polymers. *Chem. Commun.* **2017**, 53, 2463-2466.
17. Bera, D.; Hou, Z.; Glassner, M.; Lyskawa, J.; Malfait, A.; Woisel, P.; Hoogenboom, R. Supramolecular competitive host-guest interaction induced reversible macromolecular metamorphosis. *Macromol. Rapid Commun.* **2019**, 40, 1900376
18. Wang, D.; Su, Y.; Jin, C.; Zhu, B.; Pang, Y.; Zhu, L.; Liu, J.; Tu, C.; Yan, D.; Zhu, X., Supramolecular copolymer micelles based on the complementary multiple hydrogen bonds of nucleobases for drug delivery. *Biomacromolecules* **2011**, 12, 1370-1379.
19. Dong, R.; Zhou, Y.; Huang, X.; Zhu, X.; Lu, Y.; Shen, J., Functional supramolecular polymers for biomedical applications. *Adv. Mater.* **2015**, 27, 498-526.

20. Hu, X.-Y.; Liu, X.; Zhang, W.; Qin, S.; Yao, C.; Li, Y.; Cao, D.; Peng, L.; Wang, L., Controllable construction of biocompatible supramolecular micelles and vesicles by water-soluble phosphate pillar [5, 6] arenes for selective anti-cancer drug delivery. *Chem. Mater.* **2016**, *28*, 3778-3788.
21. Zhou, Y.; Jie, K.; Huang, F., A dual redox-responsive supramolecular amphiphile fabricated by selenium-containing pillar [6] arene-based molecular recognition. *Chem. Commun.* **2018**, *54*, 12856-12859.
22. Yang, K.; Chang, Y.; Wen, J.; Lu, Y.; Pei, Y.; Cao, S.; Wang, F.; Pei, Z., Supramolecular vesicles based on complex of trp-modified pillar [5] arene and galactose derivative for synergistic and targeted drug delivery. *Chem. Mater.* **2016**, *28*, 1990-1993.
23. Zhang, H.; Liu, Z.; Zhao, Y., Pillararene-based self-assembled amphiphiles. *Chem. Soc. Rev.* **2018**, *47*, 5491-5528.
24. Feng, W.; Jin, M.; Yang, K.; Pei, Y.; Pei, Z., Supramolecular delivery systems based on pillararenes. *Chem. Commun.* **2018**, *54*, 13626-13640.
25. Chi, X.; Yu, G.; Shao, L.; Chen, J.; Huang, F., A dual-thermoreponsive gemini-type supra-amphiphilic macromolecular [3] pseudorotaxane based on pillar [10] arene/paraquat cooperative complexation. *J. Am. Chem. Soc.* **2016**, *138*, 3168-3174.
26. Yu, G.; Zhao, R.; Wu, D.; Zhang, F.; Shao, L.; Zhou, J.; Yang, J.; Tang, G.; Chen, X.; Huang, F., Pillar [5] arene-based amphiphilic supramolecular brush copolymers: Fabrication, controllable self-assembly and application in self-imaging targeted drug delivery. *Polym. Chem.* **2016**, *7*, 6178-6188.
27. Rui, L.; Liu, L.; Wang, Y.; Gao, Y.; Zhang, W., Orthogonal approach to construct cell-like vesicles via pillar [5] arene-based amphiphilic supramolecular polymers. *ACS Macro Lett.* **2015**, *5*, 112-117.
28. Wang, S.; Yao, C.; Ni, M.; Xu, Z.; Cheng, M.; Hu, X.-Y.; Shen, Y.-Z.; Lin, C.; Wang, L.; Jia, D., Thermo-and oxidation-responsive supramolecular vesicles constructed from self-assembled pillar [6] arene-ferrocene based amphiphilic supramolecular diblock copolymers. *Polym. Chem.* **2017**, *8*, 682-688.
29. Yu, G.; Yu, W.; Shao, L.; Zhang, Z.; Chi, X.; Mao, Z.; Gao, C.; Huang, F., Fabrication of a targeted drug delivery system from a pillar [5] arene-based supramolecular diblock copolymeric amphiphile for effective cancer therapy. *Adv. Funct. Mater.* **2016**, *26*, 8999-9008.
30. Laggoune, N.; Delattre, F.; Lyskawa, J.; Stoffelbach, F.; Guigner, J.-M.; Ruellan, S.; Cooke, G.; Woisel, P., Synthesis, binding and self-assembly properties of a well-defined pillar [5] arene end functionalised polydimethylacrylamide. *Polym. Chem.* **2015**, *6*, 7389-7394.

31. Liao, X.; Guo, L.; Chang, J.; Liu, S.; Xie, M.; Chen, G., Thermoresponsive AuNPs stabilized by pillararene-containing polymers. *Macromol. Rapid Commun.* **2015**, *36*, 1492-1497.
32. Boursier, T.; Georges, S.; Mosquet, M.; Rinaldi, D.; d'Agosto, F., Synthesis of poly (N-acryloylmorpholine) macromonomers using RAFT and their copolymerization with methacrylic acid for the design of graft copolymer additives for concrete. *Polym. Chem.* **2016**, *7*, 917-925.
33. Chi, X.; Yu, G.; Ji, X.; Li, Y.; Tang, G.; Huang, F., Redox-responsive amphiphilic macromolecular [2] pseudorotaxane constructed from a water-soluble pillar [5] arene and a paraquat-containing homopolymer. *ACS Macro Lett.* **2015**, *4*, 996-999.
34. Grossen, P.; Witzigmann, D.; Sieber, S.; Huwyler, J., PEG-PCL-based nanomedicines: A biodegradable drug delivery system and its application. *J. Controlled Release* **2017**, *260*, 46-60.
35. Gan, L.; Goh, N.; Chen, B.; Chu, C.; Deen, G. R.; Chew, C. J. E. p. j., Copolymers of N-acryloyl-N'-methylpiperazine and methyl methacrylate: Synthesis and its application for Hg (II) detection by anodic stripping voltammetry. *Eur. Polym. J.* **1997**, *33*, 615-620.
36. Sobotta, F. H.; Hausig, F.; Harz, D. O.; Hoepfener, S.; Schubert, U. S.; Brendel, J. C., Oxidation-responsive micelles by a one-pot polymerization-induced self-assembly approach. *Polym. Chem.* **2018**, *9*, 1593-1602.
37. Moad, G.; Rizzardo, E.; Thang, S. H., Living radical polymerization by the RAFT process – A third update. *Aust. J. Chem.* **2012**, *65*, 985-1076.
38. Wu, X.; Gao, L.; Sun, J.; Hu, X.-Y.; Wang, L., Stable pillar [5] arene-based pseudo [1] rotaxanes formed in polar solution. *Chin. Chem. Lett.* **2016**, *27*, 1655-1660.
39. Wei, P.; Götz, S.; Schubert, S.; Brendel, J. C.; Schubert, U. S., Accelerating the acidic degradation of a novel thermoresponsive polymer by host–guest interaction. *Polym. Chem.* **2018**, *9*, 2634-2642.
40. Chen, Y.; Rui, L.; Liu, L.; Zhang, W., Redox-responsive supramolecular amphiphiles based on a pillar [5] arene for enhanced photodynamic therapy. *Polym. Chem.* **2016**, *7*, 3268-3276.
41. Lv, S.; Wu, Y.; Cai, K.; He, H.; Li, Y.; Lan, M.; Chen, X.; Cheng, J.; Yin, L., High drug loading and sub-quantitative loading efficiency of polymeric micelles driven by donor–receptor coordination interactions. *J. Am. Chem. Soc.* **2018**, *140*, 1235-1238.
42. Nicolai, T.; Colombani, O.; Chassenieux, C., Dynamic polymeric micelles versus frozen nanoparticles formed by block copolymers. *Soft Matter* **2010**, *6*, 3111-3118.
43. Fu, Z.; Li, L.; Wang, M.; Guo, X., Size control of drug nanoparticles stabilized by mPEG-b-PCL during flash nanoprecipitation. *Colloid Polym. Sci.* **2018**, *296*, 935-940.
44. Tao, J.; Chow, S. F.; Zheng, Y., Application of flash nanoprecipitation to fabricate poorly water-soluble drug nanoparticles. *Acta Pharm. Sin.* **2019**, *9*, 4-18.

45. He, J.; Chen, J.; Lin, S.; Niu, D.; Hao, J.; Jia, X.; Li, N.; Gu, J.; Li, Y.; Shi, J., Synthesis of a pillar [5] arene-based polyrotaxane for enhancing the drug loading capacity of PCL-based supramolecular amphiphile as an excellent drug delivery platform. *Biomacromolecules* **2018**, *19*, 2923-2930.
46. He, J.; Liu, X.; Niu, D.; Chen, J.; Qin, X.; Li, Y., Supramolecular-based PEGylated magnetic hybrid vesicles with ultra-high transverse relaxivity. *Appl. Mater. Today* **2018**, *11*, 238-245.
47. He, J.; Chen, J.; Niu, D.; Jia, X.; Wang, Q.; Hao, J.; Gu, J.; Li, Y.; Shi, J., GSH/pH dual-responsive supramolecular hybrid vesicles for synergistic enzymatic/chemo-tumor therapy. *Appl. Mater. Today* **2019**, 100458.
48. Song, W.; Tang, Z.; Lei, T.; Wen, X.; Wang, G.; Zhang, D.; Deng, M.; Tang, X.; Chen, X., Stable loading and delivery of disulfiram with mPEG-PLGA/PCL mixed nanoparticles for tumor therapy. *Nanomedicine: NBM* **2016**, *12*, 377-386.
49. Deirram, N.; Zhang, C.; Kermaniyan, S. S.; Johnston, A. P.; Such, G. K., pH-Responsive Polymer Nanoparticles for Drug Delivery. *Macromol. Rapid Commun.* **2019**, *40*, 1800917.
50. Meng, F.; Cheng, R.; Deng, C.; Zhong, Z., Intracellular drug release nanosystems. *Mater. Today* **2012**, *15*, 436-442.
51. Gan, Z.; Fung, J. T.; Jing, X.; Wu, C.; Kuliche, W., A novel laser light-scattering study of enzymatic biodegradation of poly (ϵ -caprolactone) nanoparticles. *Polymer* **1999**, *40*, 1961-1967.
52. Hu, Y.; Jiang, Z.; Chen, R.; Wu, W.; Jiang, X., Degradation and degradation-induced re-assembly of PVP-PCL micelles. *Biomacromolecules* **2010**, *11*, 481-488.
53. Geng, Y.; Discher, D. E., Hydrolytic degradation of poly (ethylene oxide)-block-polycaprolactone worm micelles. *J. Am. Chem. Soc.* **2005**, *127*, 12780-12781.
54. Chawla, J. S.; Amiji, M. M., Biodegradable poly (ϵ -caprolactone) nanoparticles for tumor-targeted delivery of tamoxifen. *Int. J. Pharm.* **2002**, *249*, 127-138.
55. Carbone, K.; Casarci, M., A New immobilization system for candida rugosa lipase: characterization and applications. *Prog. Biotechnol.* **1998**, *15*, 553-558.
56. Shen, C.; Guo, S.; Lu, C., Degradation behaviors of monomethoxy poly (ethylene glycol)-b-poly (ϵ -caprolactone) nanoparticles in aqueous solution. *Polym. Adv. Technol.* **2008**, *19*, 66-72.
57. Otero, C.; Rúa, M. L.; Robledo, L., Influence of the hydrophobicity of lipase isoenzymes from *Candida rugosa* on its hydrolytic activity in reverse micelles. *FEBS Lett.* **1995**, *360*, 202-206.

58. Tsuchiya, T., Studies on the standardization of cytotoxicity tests and new standard reference materials useful for evaluating the safety of biomaterials. *J. Biomater. Appl.* **1994**, 9, 138-157.

TOC

